RESEARCH INTO THE GRADING METHOD OF KIWI FRUIT BASED ON VOLUME ESTIMATION AND SURFACE DEFECT
/
基于体积估计和表面缺陷的猕猴桃分级方法

Prof. Ph.D. Lijia Xu [1], Stud. Yu Feng [1], Stud. Zhangkun Fan [1], Ph.D. Dingchun Yun [2]
[1] College of Mechanical and Electrical Engineering, Sichuan Agriculture University, Ya'an / China,
[2] University of Applied Sciences Upper Austria, Softwarepark 11, Hagenberg / Austria
Tel: 0835-2882035; E-mail: lijiaxu13@163.com

Abstract: *Kiwi fruit grading is a key link of fruit treatment after picking. In respect that low sorting rate and grading rate of kiwi fruits affect commodity value in China, the paper acquires the volumetric characteristic of kiwi fruit through the 3D reconstruction of its three views, and fits volumetric pixel P with actual weight W to get a mathematical model between the two parameters, and identifies the area characteristic of the surface defect of kiwi fruit by iterative method. Volumetric characteristic and the characteristic of the surface defect are inputted into Support Vector Machine (SVM), and then suitable kernel function and kernel parameters are selected, finally the kiwi fruit grading accuracy of 97.73% is gotten. Compared with the grading accuracy of BP network with 92.11%, it can be seen that the grading effect of SVM is better than that of BP network and its grading performance is stable. The experimental results show that the SVM grading method based on kiwi fruit volume and its surface defect is feasible and can be used for online inspection of appearance quality of kiwi fruits.*

摘要: *猕猴桃分级是水果产后处理的重要环节，针对中国猕猴桃分选率和分级率低而影响商品价值现状，本文通过对猕猴桃三视图进行三维重建得到猕猴桃体积特征，拟合体积像素P和实际重量W，得到两者之间的数学模型；根据迭代法切割得到猕猴桃表面缺陷面积特征。将体积特征和表面缺陷特征输入支持向量机 SVM，通过选择合适的核函数和核参数，得到猕猴桃的分级正确率为 97.73%。对比 BP 网络分级的正确率 92.11%，可知 SVM 比 BP 网络的分级效果好且 SVM 的分级性能稳定。实验结果表明基于猕猴桃体积和表面缺陷的 SVM 分级方法可行，可用于猕猴桃外部品质在线检测。*

Keywords: *Kiwi fruit grading; SVM; BP neural network; Image processing; Agricultural technology extension*

关键词: *猕猴桃分级；SVM；BP 神经网络；图像处理；农业技术推广*

INTRODUCTION

At present, the kiwi fruit grading of China mainly depends on artificial way to complete it, so both the grading efficiency and the grading accuracy are low. China has the largest production of kiwi fruits. With the increasing import and export volume of kiwi fruit year by year, the low price of kiwi fruits needs to be changed in a short time. So it is very important to improve the grading technical for kiwi fruits, which can produce more economic benefits and significantly improve its market competitiveness.

With the development of machine vision in recent years, many scholars at home and broad have developed a number of methods for quality inspection of kiwi fruit, e.g., Lü Q [3] developed detection of hidden bruise on kiwi fruit using hyperspectral imaging and parallelepiped classification, and the experimental result showed the error with 14.5% for internal damage detection by high spectrum. Wijithunga et al. [5] studied kiwi fruit detection based on generalized color picture segmentation. Yongjie [1] advanced a surface detection method for kiwi fruit grading. Wu Tao et al. [7] studied the object extraction of kiwifruit based on machine vision. While there are rare studies on external inspection and grading methods for kiwi fruits. Hence the paper developed a grading method for kiwi fruits, which used SVM as the classifier. The method can achieve the accuracy grading results for kiwi fruits according to volume estimation and surface defect.

引言

目前，猕猴桃分级的中国主要依靠人工的方式来完成，分类效率和分类精度都比较低。中国拥有最大生产的猕猴桃生产基地。每年随着越来越多的猕猴桃进口和出口量，猕猴桃价格偏低的现象急需在较短的一段时间内改变。所以提高猕猴桃分级的技术非常重要，它能够产生很好的经济效益，提高其市场竞争力。

近年来，随着机器视觉的发展，国内外学者做了许多关于猕猴桃品质检测的方法，如吕强等[3] 利用高光谱图像检测猕猴桃内部损伤，其实验结果表明高光谱检测内部损伤的误差为 14.5%；P. Wijithunga 等[5]研究了基于广义彩色图像分割的猕猴桃检测方法；崔永杰等[1]提出了猕猴桃分级果实表面缺陷的检测方法；武涛等[7]做了基于机器视觉的猕猴桃果实目标提取研究。综上所述可知对猕猴桃外部检测并进行分级的研究较少，对此，本文研制了一种基于猕猴桃体积估计和表面缺陷的分级方法，以 SVM 作为分类器，并根据猕猴桃等级规格，实现了基于体积估计和表面缺陷的猕猴桃准确分级。

MATERIAL AND METHOD

Feature Extraction of Kiwi Fruit

Usually a picture shot by the camera is noisy, so it needs pre-processing [10]. Picture of Kiwi fruit snapped

材料与方法

猕猴桃的特征提取

通常摄像头拍摄的图像存在噪声，故需要对图像进行预

by camera is shown in Fig. 1(a), and the original picture is transferred from RGB space into the second channel (saturation) in HSV space, as shown in Fig. 1(b). Picture with median filtering for Fig. 1(b) is shown in Fig. 1(c), from which it can be seen that the picture has strong contrast, less fuzziness and complete edge information. Edge extracting is conducted by canny operator for Fig. 1(c), and the result is shown in Fig. 1(d). Fig. 1(e) is obtained through the expansion of Fig. 1(d), and then Fig. 1(f) is gotten through the fill in Fig. 1(e). Later the region picture of kiwi fruit is acquired through corrosion, open operation, redundant pixel deletion and other operations for Fig. 1(f), as shown in Fig. 1(g). Then Fig. 1(g) is viewed as formwork and inverted, finally logical product is conducted for R, G and B components of the picture shown in Fig. 1(a) to get kiwi fruit picture divided from the background, as shown in Fig. 1(h).

处理 [10]。摄像头拍摄的猕猴桃图像如图 1(a) 所示，将原始图像从 RGB 空间转换为 HSV 空间的第二通道(饱和度)如图 1(b)所示。对图 1(b)进行中值滤波处理的图像如图 1(c), 可知图 1(c)的对比度强，模糊少，边缘信息保存较完整。对图 1(c) 用 canny 算子进行边缘提取，结果如图 1(d)。对图 1(d)进行膨胀处理得图 1(e)，再对图 1(e)进行填充得图 1(f)，继而对图 1(f)进行腐蚀、开运算和删除冗余像素等操作后，获得猕猴桃的区域图像如图 1(g)。将图 1(g) 作为模板并取反，与图 1(a)所示图像的 R、G、B 分量进行与运算，得到从背景中分割出来的猕猴桃图像如图 1(h)。

(a) (b) (c) (d) (e) (f) (g) (h)

Fig. 1 - Picture pre-processing process

(a) Kiwi fruit picture (b) Saturation picture (c) Median filtering picture (d) Canny edge extracting picture (e) Expansion picture (f) Fill picture (g) Region picture of Kiwi fruit (h) Division picture of Kiwi fruit

Extraction of volumetric feature

Volume is a key indicator in many fields, and a very important feature for fruit grading. Normally, the larger a fruit is, the heavier it will be. The paper designs a volume measuring method of the kiwi fruit based on computer vision.

After the pre-processing of 3 views of the kiwi fruit picture, all of its front view, side view and top view are in 100×100 pixels, as shown in Fig. 2(a-c). Front view is read in to calculate its edge, as shown in Fig. 2(d), and the coordinates of 4 orientation points locating at the easternmost, the westernmost, the northernmost and the southernmost areas respectively among the edge contour points of the front view are found out. Side view is read in to calculate its edge, and the coordinates of 4 orientation points in the easternmost, the westernmost, the northernmost and the southernmost respectively among the edge contour points of side view are found out. Taking the edge of the front view as the benchmark, the edge position of the side view is adjusted to align the horizontal coordinate of the northernmost orientation point among the edge contour points of the side view with that of the northernmost orientation point among the edge contour points of the front view, and the result is shown in Fig. 2(e). Top view is read in to calculate its edge, and then its edge position is adjusted as per the coordinates of 4 orientation points on the edge of the front view and those of 4 orientation points on the edge of the adjusted side view, so that the horizontal coordinate of the northernmost orientation point among the edge contour points of the top view is corresponding to the ordinate of the easternmost orientation point among the edge contour points of the side view. Similarly, the edge of the top view is adjusted so that the ordinate of the westernmost orientation point among its edge contour points is corresponding to that of the westernmost orientation point among the edge contour points of the front view, and the result is shown in Fig. 2(f). The coordinates of the 4 orientation points in the easternmost, the westernmost, the northernmost and the southernmost among the edge contour points of the adjusted top view are achieved to find out the center point of the top view's edge further.

体积特征的提取

在许多领域中体积是一个重要的指标，在水果分级中它更是一个非常重要的特征，一般而言，体积越大则重量越大。本文设计了基于计算机视觉的猕猴桃体积测量方法。

对猕猴桃的三视图进行预处理后，使其正视图、侧视图和俯视图都为100 × 100像素，如图 2(a-c)所示。读入正视图，求取正视图边缘，如图 2(d)，找到正视图边缘轮廓点中的最东面、最西面、最北面和最南面的 4 个方位点的坐标；读入侧视图，求取侧视图边缘，找到侧视图边缘轮廓点中的最东面、最西面、最北面和最南面的 4 个方位点的坐标。以正视图边缘为标准，调整侧视图边缘的位置，使其边缘轮廓点中的最北面方位点的横坐标与正视图边缘轮廓点中的最北面方位点的横坐标相对准，结果如图 2(e)所示。读入俯视图，求取俯视图边缘，以正视图边缘 4 个方位点坐标和调整后的侧视图边缘 4 个方位点坐标为参照，调整俯视图边缘的位置，使其边缘轮廓点中的最北面方位点的横坐标对应侧视图边缘轮廓点中的最东面方位点的纵坐标；同理，调整俯视图边缘使其边缘轮廓点中的最西面方位点的纵坐标与正视图边缘轮廓点中的最西面方位点的纵坐标相对应，结果如图 2(f)。获得调整后俯视图边缘轮廓点中的最东面、最西面、最北面和最南面的 4 个方位点的坐标，利用此 4 个方位点的坐标找到俯视图边缘的中心点。

(a) (b) (c) (d) (e) (f)

Fig. 2 - Three views and edges of all adjusted views of kiwi fruit
(a) Front view (b) Side view (c) Top view (d) Edge of adjusted front view (e) Edge of adjusted side view (f) Edge of adjusted top view

Creating $100 \times 100 \times 100$ cube zero matrix named as $KJ1$. Edges of the front view, edges of the side view and edges of the top view are adjusted to correspond to the front, side and top of $KJ1$, respectively. Taking the ordinate i_1 of the westernmost orientation point among the edge contour points of the side view as the initial point and the ordinate i_n of the easternmost one as the end point, the edge of the front view is copied to Layer i_x of $KJ1$ to get $KJ1(:, i_x, :)$, $i_x \in (i_1, i_2, \cdots, i_x, \cdots, i_{n-1}, i_n)$. Taking the ordinate j_1 of the easternmost orientation point among the edge contour points of front view as the initial point and the ordinate j_n of the westernmost one as the end point, $KJ1(j_x, :, :)$, $j_x \in (j_1, j_2, \cdots, j_x, \cdots, j_{n-1}, j_n)$ are transposed and further assigned to 100×100 square zero matrix named as QP. Aligning QP with the center point of the side view's edge and then conducting overlap, the results are shown in Fig. 3(a-c). Then the coordinate (x_z, y_z), $z \in (1 \cdots \omega)$ of the edge contour points of their intersection can be found out, where ω is number of edge contour points. Clearing the j_x Layer of $KJ1$, i.e., $KJ1(j_x, :, :)$ and assigning $KJ1(j_x, x_z, y_z)$ to 1, the slice set of edge of side view can be obtained through traversing all j_x values, as shown in Fig. 3(d-f).

创建$100 \times 100 \times 100$的正方体零矩阵$KJ1$。将正视图边缘对应$KJ1$的正面，侧视图边缘对应$KJ1$的侧面，俯视图边缘对应$KJ1$的上面。以侧视图边缘轮廓点中的最西面方位点的纵坐标i_1为起点，最东面方位点的纵坐标i_n为终点，将正视图边缘复制在$KJ1$的第i_x层上得到$KJ1(:, i_x, :)$，$i_x \in (i_1, i_2, \cdots, i_x, \cdots, i_{n-1}, i_n)$。以正视图边缘轮廓点中的最东面方位点的纵坐标$j_1$为起点，最西面方位点的纵坐标$j_n$为终点,将$KJ1(j_x, :, :)$，$j_x \in (j_1, j_2, \cdots, j_x, \cdots, j_{n-1}, j_n)$转置后赋给$100 \times 100$的正方形零矩阵$QP$。 将$QP$和侧视图边缘的中心点对准后进行叠加，叠加图如图 3(a-c)所示。从而可以找到两者交集部分的边缘轮廓点的坐标(x_z, y_z), $z \in (1 \cdots \omega)$，ω为边缘轮廓点数。将上述$KJ1$的第j_x层$KJ1(j_x, :, :)$清零，再将$KJ1(j_x, x_z, y_z)$赋值为 1，遍历完所有j_x值得到侧视边缘切片集，如图 3(d-f)所示。

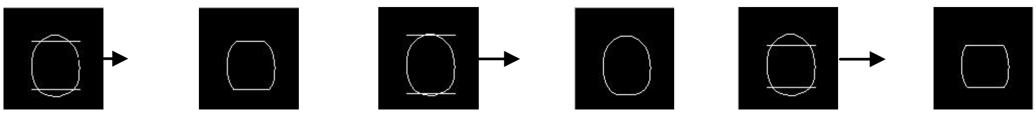

(a) (d) (b) (e) (c) (f)

Fig. 3 - Edge cutting effect graph of side view
(a) Overlap picture 1 (b) Overlap picture 2 (c) Overlap picture 3
(d) Slice 1 of side view (e) Slice 2 of side View (f) Slice 3 of side view

In $KJ1(:, :, k_x)$, different k_x values correspond to different rectangular slices, thereof, $k_x \in (k_1, k_2, \cdots, k_x, \cdots, k_{n-1}, k_n)$. k_1 is the horizontal coordinate of the northernmost orientation point among the edge contour points of the front view, and k_n is that of the southernmost one. Schematic graphs of different rectangular slices are shown in Fig. 4(a-c).

在$KJ1(:, :, k_x)$中不同k_x对应不同的矩形切片，其中，$k_x \in (k_1, k_2, \cdots, k_x, \cdots, k_{n-1}, k_n)$。$k_1$为正视图边缘轮廓点中的最北面方位点的横坐标，$k_n$为正视图边缘轮廓点中的最南面方位点的横坐标。不同矩形切片示意图如图 4(a-c)所示。

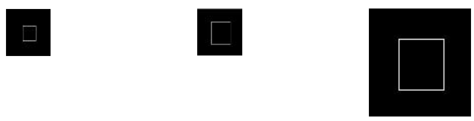

(a) (b) (c)

Fig. 4 - Schematic graphs of rectangular slices

After traversing all rectangular slices, the minimum ordinates of contour points of each layer of rectangular slices are saved in array named as *M*. Then the maximum and minimum in *M* are found out, and the absolute value of their difference is viewed as the minification base number. Taking k_1 and k_n as the initial and end point respectively, the rectangular slice of k_x Layer, i.e., $KJ1(:,:,k_x)$, is transposed and further exchanged vertically, and then assigned to matrix named as *N*. Subtracting the minimum ordinate value of rectangular slice contour points in *N* by the minimum in *M*, and the quotient of dividing the absolute value of their difference by the minification base number is viewed as minification λ of the k_x layer edge of top view, i.e.

遍历完所有矩形切片，将各层矩形切片轮廓点中的最小纵坐标存放在数组 M 中。找到 M 中的最大值和最小值，将两者相减的绝对值作为缩小倍数基数。以 k_1、k_n 分别作为起点和终点，将第 k_x 层的矩形切片 $KJ1(:,:,k_x)$ 转置并上下交换后赋给矩阵 *N*。将 *N* 所述矩形切片轮廓点中的最小纵坐标值与 M 中的最小值相减，相减后的差值的绝对值和缩小倍数基数相除的结果作为第 k_x 层俯视图边缘缩小的倍数 λ，即：

$$\lambda = \frac{|\min(N) - \min(M)|}{|\max(M) - \min(M)|} \tag{1}$$

Edges of the top view are contracted by double interpolation algorithm [2] according to minification number λ, and the contracted picture matrix is further expanded into 100×100 matrix. During the expansion process, the coordinates of each point of the original picture matrix remain, and all new expanded points are filled by 0. Center point of the contracted picture is aligned with that of edge of the top view to get matrix named as *L*. The center points of *L* and *N* are aligned and overlapped to get matrix named as *S*, as shown in Fig. 5(a) and 5(c). In *S*, the intersection between *L* and *N* is defined as boundary. The center point of *S* is found out by the coordinates of the easternmost, the westernmost, the southernmost and the northernmost orientation points in *S*. Such center point will be rounded into an integer if it isn't an integer, and viewed as the initial growing coordinate [6]. Starting from these initial growing points, the growth spreads to all directions in *S* till the coordinates of all growing initial points and the points (x_m, y_m) within it and the boundary whose values are equal to 0 are found out, where, $m = 1 \cdots \psi$, ψ is number of all points equaling to 0 therein. $100 \times 100 \times 100$ cube zero matrix $KJ2$ is created, and all elements of $KJ2(y_m, x_m, k_x)$ are assigned with 1. Regional growing slice sequence graph can be achieved after all $k_x \in (k_1, k_2, \cdots, k_x, \cdots, k_{n-1}, k_n)$ values are traversed, where different k_x values correspond to different regional growing slices, as shown in Fig. 5(b) and Fig.5(d).

利用双插值算法[2]对俯视图边缘按照倍数 λ 进行缩小，将缩小后的图像矩阵进一步扩展为 100×100 的矩阵。在扩展过程中，原图像矩阵各点的坐标不变，新扩展的点则全部用 0 来填充。将缩小后的图像的中心点和俯视图边缘的中心点对准得到矩阵 *L*。将 *L* 和 *N* 的中心点对准后进行叠加得到矩阵 *S*，*S* 如图 5(a)和图 5(c)。在 *S* 中将 *L* 和 *N* 的交集部分定义为边界.利用 *S* 中的最东面、最西面、最南面和最北面方位点的坐标找到 *S* 的中心点，若该中心点不为整数则将其化为整数，以此中心点作为生长起始坐标 [6]。从该生长起始点开始，在 *S* 中向四面生长，直到找完包括生长起始点在内的生长起始点和边界之间所有值为 0 的点的坐标 (x_m, y_m), $m = 1 \cdots \psi$，ψ 为生长起始点和边界之间所有值为 0 的点的个数。创建 $100 \times 100 \times 100$ 的正方体零矩阵 $KJ2$，将所有 $KJ2(y_m, x_m, k_x)$ 赋值为 1，遍历完所有 $k_x \in (k_1, k_2, \cdots, k_x, \cdots, k_{n-1}, k_n)$ 值即得到区域生长切片序列图，不同 k_x 对应不同区域生长切片如图 5(b)和图 5(d)。

(a) (b) (c) (d)

Fig. 5 - Schematic graphs of *S* and region growing slice

(a) Schematic graph 1 of *S;* (b) Schematic graph 1 of region growing slice; (c) Schematic graph 2 of *S;* (d) Schematic graph 2 of region growing slice

All points equaling to 1 in $KJ2$ are drawn by MATLAB to get the 3D scatter graph of kiwi fruit, and statistics is made for the number of 1 in $KJ2$ to get the pixel numbers of 3D scatter graph of kiwi fruit named as P, which is also used as volumetric feature of kiwi fruit. The 3D scatter graph of kiwi fruit is shown in Fig. 6.

利用 MATLAB 绘制出 $KJ2$ 中所有值为 1 的点即得到猕猴桃的立体三维散点图，统计 $KJ2$ 中 1 的个数即可得到猕猴桃立体三维散点图的像素个数 P，P 即作为猕猴桃的体积特征。猕猴桃的三维散点图如图 6 所示。

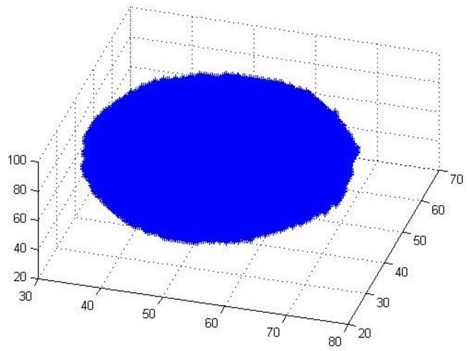

Fig. 6 - 3D Scatter graph of kiwi fruit

Abstraction of surface defect characteristic

Surface defects of kiwi fruit mainly include scrape, bruise, press, sunburn [8]. First, kiwi fruit is transferred from RGB space to HSV space, and then kiwi fruit picture is abstracted from the background of original picture in the saturation channel. The abstracted picture is cut to get Fig. 7(a), and then the gray scale chart of the cut picture is obtained, as shown in Fig. 7(b). Gray scale transformation is made for the gray scale chart, and the contrast of such chart is intensified to get Fig. 7(c). Fig.7(c) is divided by optimal threshold T_2 to get Fig. 7(d), and the threshold is calculated by iterative method. Defect detection is conducted for Fig.7(d) by canny operator with the threshold of 0.79 to get canny division graph shown in Fig. 7(e). Edge in Fig. 7(e) is removed to get Fig. 7(f), and defect in Fig. 7(f) is filled to get Fig. 7(g). Finally, Fig.7(g) is restored to get defect color graph shown in Fig. 7(h). Defect area of kiwi fruit in Fig. 7(g) is calculated as the surface defect feature of kiwi fruit.

表面缺陷特征的提取

猕猴桃表面缺陷主要有划伤、碰压伤和日灼缺陷等[8]。首先，将猕猴桃由 RGB 空间转换为 HSV 空间，在 HSV 空间的饱和度通道中将对猕猴桃图像从原始图像的背景中提取出来。对提取出来的猕猴桃裁剪得到图 7(a)，求取裁剪图的灰度图如图 7(b)；对灰度图进行灰度变换，增强灰度图的对比度得到图 7(c)；将灰度变换图 7(c)用最佳阀值 T_2 分割得到图 7(d)，最佳阀值采用迭代法求取；利用 canny 算子对图 7(d)进行缺陷检测，其中 canny 算子的参数阀值设置为 0.79，得到图 7(e)所示的 canny 分割图；对图 7(e)去除边缘得到图 7(f)；对图 7(f)填充其缺陷得到图 7(g)；最后对图 7(g)进行复原得到缺陷彩色图 7(h)；计算图 7(g)中猕猴桃的缺陷面积并作为猕猴桃表面缺陷特征。

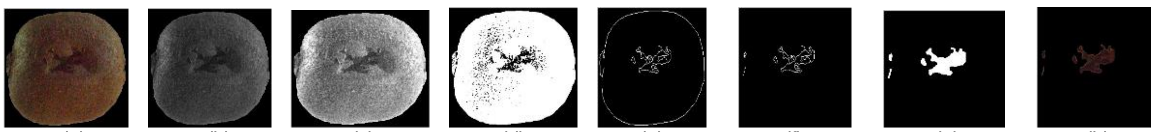

(a) (b) (c) (d) (e) (f) (g) (h)

Fig. 7 - Defect characteristic abstraction graph of iterative method
(a) Tailed graph; (b) Gray scale chart; (c) Gray scale transformation graph; (d) Iterative effect graph; (e) Canny division graph; (f) Edge removal graph; (g) Defect fill graph; (h) Defect color graph

RESULTS AND ANALYSIS

Weight Estimation

Total 40 kiwi fruits in different sizes, regular shape, the same variety and the same batch are randomly selected as sample. The volumetric pixel with $P/1000$ is fitted with actual weight W by least square method, and the result is shown in Figure. 8.

实验结果和分析

重量估计

随机选取 40 个大小不一且形状规则的同品种同批次的猕猴桃作为样本，用最小二乘法拟合猕猴桃的体积像素 $P/1000$ 与重量 W 的关系，拟合结果如图 8 所示。

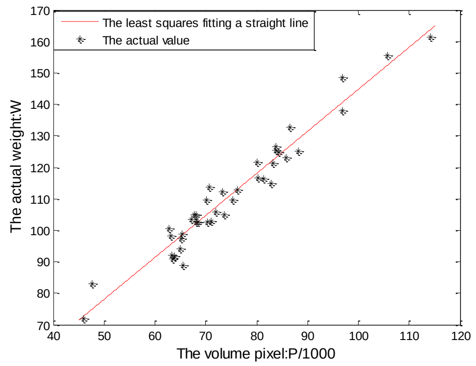

Fig.8 - Graph of relation for fitting of volumetric pixel with weight

According to experimental data, the relation between volumetric pixel $P/1000$ (unit: piece) and weight W (unit: g) of kiwi fruit is shown as follow:

经实验数据得出猕猴桃的体积像素值$P/1000$（单位：个)与其重量W（单位：g)之间的关系为：

$$W = \frac{1.3350 \times p + 11.2655}{1000} \quad (2)$$

Analysis of variance for weight W and volumetric pixel P is shown in Table 1, in which the testing value $F > (F_\alpha = F_{0.01}(1, n-2))$. The value of F shows that the influence is highly significant. The coefficient of determination r is shown as follow:

重量W与体积像素 P 的方差分析如表 1 所示，其中，检验值$F > (F_\alpha = F_{0.01}(1, n-2))$故为高度显著，可决系数$r$为：

$$r^2 = \frac{SSR}{SST} = 0.9501 \quad (3)$$

In the formula, the sum of squared residuals (SSR) is the sum of squares of residuals, and the total sum of squares (SST) is defined as being the sum, over all observations, of the squared differences of each observation from the overall mean.

The result that the value of r is approximate to 1 shows good regression effect when using volumetric pixel P of kiwi fruit to estimate its weight W. Moreover, weight of kiwi fruit W is in positive correlation with its volumetric pixel P. The more volumetric pixel P is, then the larger weight W will be. Standard error S_y is shown as follow:

式中，SSR代表回归值与均值的总离差平方和，SST代表观测值与均值的总离差平方和。

可决系数r接近 1，表明用猕猴桃的体积像素 P 估计其重量 W 的回归效果良好。猕猴桃的重量 W 和体积像素 P 成正相关性，体积像素越大，实际重量越大。标准误差S_y为：

$$S_y = \sqrt{\frac{SSE}{n-2}} = 4.2490 \quad (4)$$

In the formula, $SSE = SST - SSR$, and n means the number of kiwi fruits. The value of S_y shows small error and validates the effectiveness of the model, i.e., formula. (2).

式中，$SSE = SST - SSR$, n代表猕猴桃个数。S_y的计算结果表明误差偏小，验证了本模型即式（2）的可行性。

Table 1

Analysis of variance for actual weight and volumetric pixel

Source of variance	*Ssd*	*Df*	*Va*	*F*	*Fa*	*Significance*
Regression	13052	1	13052	722.93	4.098	Highly Significant
Residual	686.06	8	18.054		7.352	
Total	13738	9				

Total 20 kiwi fruits in different sizes, regular shape, the same variety and the same batch are randomly selected as sample, and their volumetric pixels are inputted into the model to get the fitted value of kiwi fruit weight. The result of comparison between the fitted values and actual weights of kiwi fruits is shown in Fig. 9.

随机选取待测猕猴桃中的 20 个大小不一且形状较规则的、同品种同批次的猕猴桃，将其体积像素输入该模型得到猕猴桃重量的拟合值，该拟合值和猕猴桃的实际重量值的比较结果如图 9 所示。

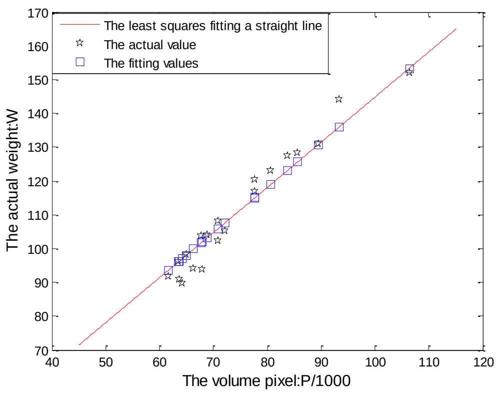

Fig.9 - Comparison graph for fitted value and actual value of kiwi fruit weight

From Fig.9, it can be seen that the fitted values of kiwi fruits weight are approximate to their actual weights, thus the model shown in formula.(2) has good regression fitting result and can be used for estimating the actual weights of kiwi fruits .

由图 9 可知，猕猴桃重量的拟合值接近其实际重量值，表明此模型回归拟合效果良好，可用于猕猴桃的实际重量估计。

Empirical classification of kiwi fruits and data preprocessing

Kiwi fruits are empirically graded into 4 grades [9]. The same variety and batch of kiwi fruits are classified into large type (marked as L), medium type (marked as m), small type (marked as S) and very small type (marked as VS) by size, and they are also classified into defect type (marked as D) and no defect type (marked as ND) by surface defect. Different classes of kiwi fruits are shown in Table 2.

猕猴桃的经验分类与数据预处理

将猕猴桃按照经验分为 4 类[9]，同品种同批次的猕猴桃按外观大小分为大(L)、中(M)、小(S)、很小（SS），按表面缺陷面积分为缺陷（D）和无缺陷(ND)，分类标准如表 2 所示。

Table 2

Grading of kiwi fruits

Grade	*Size*	*Defect*
First-class	L	ND
Second-class	M	ND
Third-class	S	ND
Fourth class	L	D
	M	D
	S	D
	VS	ND
	VS	D

Volumetric pixels and surface defect areas of total 88 kiwi fruits are selected and normalized. Different standardization methods generate different grading results. Through repetitive experiments, z-score standardization method is selected, i.e.

选择 88 个猕猴桃的体积像素和缺陷面积并将其归一化处理。不同标准化方法对分级结果有不同影响，经过反复实验选择 z-score 标准化方法，即：

$$z_{ij} = \frac{x_{ij} - \bar{x}_i}{s_i} \tag{5}$$

In the formula, z_{ij} means converted real variable value, and x_{ij} means actual variable value. $\bar{x}_i$ and s_i are arithmetic mean and standard deviation of variable, respectively.

式中，z_{ij} 为转化后的实变量值，x_{ij} 为实际变量值，$\bar{x}_i$ 和 s_i 分别是变量的算术平均值和标准差。

Grading effect of SVM

The 2 kinds of features, i.e., standardized volumetric pixel and surface defect area, are inputted into SVM with v-SVC type and SVM with c-SVC type. Different kernel functions are selected for experiment. Sample number of training set and that of testing set are 44, respectively, and the grading results are shown in Table 3.

SVM 的分级效果

将上述标准化后的体积像素和表面缺陷面积 2 类特征输入 v-SVC 型 SVM 和 c-SVC 型 SVM。选择不同核函数进行实验，训练集和测试集样本数各 44 个，分级结果如表 3 所示。

Table 3

Results of grading by different kernel functions

SVM type	Kernel function type	Grading accuracy
c-SVC	Linear kernel function	84.09%(37/44)
	Polynomial kernel function	88.64%(39/44)
	RBF kernel function	97.73%(43/44)
	Sigmoid kernel function	70.45%(31/44)
v-SVC	Linear kernel function	86.36%(38/44)
	Polynomial kernel function	88.64%(39/44)
	RBF kernel function	97.73%(43/44)
	Sigmoid kernel function	81.82%(36/44)

From Table 3, it can be seen that the highest grading accuracy of the 2 kinds of SVMs adopting RBF kernel function is 97.73%, but the SVM with v-SVC type adopting other kernel functions has a little better grading result, so all subsequent grading experiments use such SVM as the classifier and RBF as the kernel function.

SVM training is attributed to the solution of convex quadratic programming problems under linear constraint [11], and SVM will occupy large storage space when training set is large. Different training sets are inputted into SVM, and the grading results are shown in Table 4.

由表 3 可知，两类 SVM 均在选择 RBF 核函数时获得最高的分级准确率 97.73%，但选择其他核函数时 v-SVC 型 SVM 的分级效果稍高些，故后续的分级实验均是以此类 SVM 作为分类器，且选择 RBF 作为核函数。

SVM 的训练归结为求解线性约束下的凸二次规划问题[11]，当训练集较大时，SVM 将会占据较大的存储空间。将不同训练集输入 SVM ，结果如表 4 所示。

Table 4

Grading results of different training sets

Training set number	*Testing set number*	*Grading accuracy*
25	44	97.73%
30	44	97.73%
36	44	97.73%
44	44	97.73%

From Table 4, it can be seen that different numbers of training sets inputted into SVM with v-SVC type bring the same grading accuracy of 97.73%, so this type of SVM has stable grading performance and can always realize very high grading accuracy for different sample inputs.

In order to investigate the influence of kernel parameter σ of SVM on kiwi fruit grading accuracy [4], 44 training sets and 44 testing sets are selected respectively, and the grading results of SVM using different σ values are shown in Table 5.

由表 4 可知，不同训练集输入 v-SVC 型 SVM 得到相同的分级正确率 97.73%，由此可知该型 SVM 分级性能稳定，在不同样本输入的情况下均能得到很高的分级准确率。

为了考察 SVM 的核参数 σ 对猕猴桃分级正确率的影响[4]，分别选择训练集和测试集各 44 个，在 σ 取不同值时 SVM 的猕猴桃分级结果如表 5 所示。

Table 5

Grading results at different σ values

Nuclear parameters(σ)	*Grading accuracy*
0.5	93.18%
1.0	95.45%
1.5	97.73%
2.0	97.73%
3.0	97.73%
5.0	95.45%
10.0	90.91%

From Table 5, it can be seen that different σ values influence grading results greatly. SVM has optimal grading accuracy for σ distributed in the interval [1.5, 3.0]. SVM is in a state of over learning for σ <1.5 and in a state of under learning for σ >3.0.

由表 5 可知， σ 值在[1.5, 3.0]时 SVM 的分级精度达到最佳。当 σ <1.5 时，SVM 过度学习；当 σ >3.0 时，SVM 学习不足。

Grading effect of BP network

BP network is the most widely applied back propagation network. The next kiwi fruit grading experiment based on BP network will be conducted with sample numbers of training set and testing set are 50 and 38, respectively. Training times is 50 and learning velocity is 0.1. The volumetric and defect area features are inputted into BP network, so the number of input layer neurons is set to 2. Kiwi fruits have 4 grades, so BP network has 4 output layer neurons, and the grading results for different numbers of hidden layers are shown in Table 6. From Table 6, it can be seen that BP network has the grading accuracy with 92.11% for 8 hidden neurons.

BP 网络的分级效果

BP 网络是目前应用最广泛的反向传播网络。下面进行基于 BP 网络的猕猴桃分级实验，训练集、测试集样本数分别为 50 个和 38 个，训练次数为 50，学习速率为 0.1，输入层神经元个数为 2，体积特征和缺陷面积特征作为 BP 网络的输入，故其输入层神经元个数为 2，猕猴桃有 4 个等级故 BP 网络的输出层神经元个数为 4，选择不同的隐含层个数获得分类结果如表 6 所示。由表 6 可知，当隐含层神经元个数为 8 时，BP 网络的分级正确率为 92.11%。

Table 6

Grading results based of different numbers of hidden neurons

Number of hidden layer neurons	5	6	7	8	9	10
Grading accuracy	86.84%	86.84%	86.84%	92.11%	76.32 %	84.21%

Comparison of SVM and BP network in grading results

Grading experiments by SVM with v-SVC at different sample numbers of training set and that by BP network with 8 hidden neurons are conducted, and their grading results are shown in Table 7.

SVM 与 BP 网络的分级结果比较

选择在不同训练集样本数的情况下进行 v-SVC 型 SVM 和隐含层神经元个数为 8 的 BP 网络的分级实验，分级结果如表 7 所示。

Table 7

Comparison of SVM and BP network in grading results

Training set number	*Test set number*	*SVM Grading accuracy*	*BP Grading accuracy*
25	40	97.50%	82.50%
30	40	97.50%	87.50%
36	40	97.50%	90.00%
44	40	97.50%	92.50%

From Table 7, it can be seen that the grading accuracy of SVM is always 97.50% for different sample numbers of training set, while that of BP network is greatly influenced by the training sample number. Moreover, the grading accuracy of SVM is always higher than that of BP network, so SVM can also obtain higher grading accuracy for small training samples while BP network needs more training samples.

由表 7 可知，在训练集样本数不同的情况下，SVM 的分级正确率均为 97.50%，BP 网络的分级正确率则受训练样本数的影响较大，且 SVM 的分级正确率高于 BP 网络的分级准确率，这说明 SVM 在训练样本数较小时也可获得很高的分级正确率， BP 网络则需要较多的训练样本数。

CONCLUSIONS

The paper develops a grading method of kiwi fruit based on volume estimation and surface defect. Mathematical model for the weight and volumetric pixel of kiwi fruit is fitted. The coefficient of determination is 0.9501, and the standard error is 4.2490, so the model has a good fitting effect and can be used for actual weight estimation of kiwi fruits. The SVM with v-SVC type adopting RBF kernel function can obtain the grading accuracy with 97.73% under the optimal kernel parameter σ ; The grading accuracy of BP network is rising along with the increase of numbers of training sets when the optimal number of hidden layers is 8. The grading performance of SVM is superior to that of BP neural network under different numbers of training set, and the grading accuracy of SVM is always higher than that of BP neural network.

结论

本文研究了一种基于猕猴桃体积估计和表面缺陷的分级方法。本方法拟合出猕猴桃的重量和体积像素之间的数学模型，计算出可决系数为 0.9501，标准误差为 4.2490，表明该模型的拟合效果良好，可用于猕猴桃的实际重量估计。核函数为 RBF 的 v-SVC 型 SVM 在最佳核参数 σ 时其分级正确率可达 97.73%；BP 网络的最佳隐含层个数为 8，分级正确率随着训练集个数的增加而增加。在不同训练样本数下 SVM 的分级性能优于 BP 神经网络的分级性能，且其分级正确率高于 BP 网络的分级正确率。

ACKNOWLEDGEMENT

This paper was funded by the Natural Science Project of Sichuan Education Department under Grant 12ZA277.

致谢

本文受到四川省教育厅自然科学重点项目（项目号：12ZA277）。

REFERENCES

[1]. Cui Yongjie, Li Pingping, Ding Xian, et al., (2012) - *Kiwi fruit grading methods used for the detection of surface defects*, Agricultural Mechanization Research, Vol.34, No.10, pp.139-142;

[2]. Li Zhen,Hong Tiansheng,Wu Weibin, et al., (2006)- *Bilinear interpolation algorithm in the numerical simulation of litchi tree photosynthetic leaves the application of the image rotation*, Transactions of the CSAE, Vol.22, No.11, pp.179-182;

[3]. Lü Q, Tang M J., (2012) - *Detection of hidden bruise on kiwi fruit using hyperspectral imaging and parallelepiped classification*, Procedia Environmental Sciences,Vol.12, Part B, pp.1172-1179.

参考文献

[1]. 崔永杰, 李平平, 丁宪, 等., (2012)- *猕猴桃分级果实表面缺陷的检测方法*，农业机械化研究，第 34 卷，第 10 期, 139-142;

[2]. 李震, 洪添胜, 吴伟斌, 等., (2006) - *双线性差值算法在荔枝树光合模拟中叶片图像旋转中的应用*, 农业工程学报，第 22 卷, 第 11 期, 179-182;

[3]. 吕强，唐明杰., (2012)- *利用高光谱成像和平行分类检测隐藏挫伤猕猴桃*. Procedia 环境科学，第 12 卷，B 部，1172-1179;

[4]. Lin Shengliang, Liu Zhi., (2007)- *Parameter selection in SVM with RBF kernel function*, Journal of Zhejiang University of Technology, Vol. 35, No.2, pp.163-167.
[5]. P. Wijethunga, S. Samarasinghe, D. Kulasiri., (2009)- *Towards a generalized color image segmentation for kiwifruit detection*, 24th International Conference Image and Vision Computing, Wellington , New Zealand , Nov. 23-25，pp.62-66.
[6]. Shao Hehong, Zheng Wanting, et al. (2009)- *Chinese gooseberry stage division based on computer vision*, Beijing Biomedical Engineering,Vol.28,No.5, pp.531-533;
[7]. Wu Tao, Yuan Chi, Chen Jun. (2012) - *Research on the object extraction of kiwifruit based on machine vision*, Agricultural Mechanization Research, Vol.34, No.12, pp. 21-26;
[8]. Wang Junhao, Yang Wenhui. (2011) - *Common pests and Integrated Prevention of kiwifruit*, Plant Doctor, Vol.24, No.3, pp. 16-17;
[9]. Xu L., You Z., Wu S. et al., (2013) - *Development and experiment on automatic grading equipment for kiwi*, INMATEH-Agricultural Engineering, Vol.41, No.3, pp. 55-64;
[10]. Yang Jie, Huang Chaobing., (2010) - *Digital image processing and MATLAB*, Beijing: Electronic Industry Press;
[11]. Ying Wei, Wang Zhengou, An Jinglong., (2006) - *Study on Multiclass Text Categorization Method Based on Improved Support Vector Machine*, Computer Engineering, Vol.32, No.16, pp.74-76.

[4]. 林升梁. 刘志., (2007)- *基于RBF 核函数的支持向量机参数选择*, 浙江工业大学学报,第 35 卷,第 2 期,163-167;
[5]. P. Wijethunga, S. Samarasinghe, D. Kulasiri 等., (2009) - *基于广义彩色图像分割的猕猴桃检测*，第 24 届图像与视觉计算国际会议, 新西兰惠灵顿, 2009 年 11 月 23-25 日，62-66;
[6]. 邵和鸿. 郑万挺. 彭加寅.,(2009)- *基于计算机视觉技术的猕猴桃分级方法*, 北京生物医学工程, 第 28 卷, 第 5 期, 531-533;
[7]. 武涛, 袁池, 陈军., (2012) - *基于机器视觉的猕猴桃果实目标提取研究*, 农机化研究, 第 34 卷,第 12 期, 21-26;
[8]. 王筠皓. 杨文辉., (2011) - *猕猴桃常见病虫害种类及综合防治*,植物医生, 第 24 卷, 第 3 期,16-17;
[9]. 许丽佳, 游志昆, 邬盛, 等. (2013) - *猕猴桃自动分级设备的研究与应用*,农业工程,第 41 卷,第 3 期, 55-64;
[10]. 杨杰, 黄朝兵., (2010) - *数字图像处理及 MATLAB 实现*, 北京: 电子工业出版社;
[11]. 应伟, 王正欧, 安金龙., (2006) - *一种基于改进的支持向量机的多类文本分类方法*, 计算机工程, 第 32 卷,第 16 期, 74-76.